Modern Physics Letters B
Vol. 29 (2015) 1550131 (10 pages)

DOI: 10.1142/S0217984915501316

Diameter control of carbon nanotubes using argon–acetylene mixture and their application as IR sensor

Rana Arslan Afzal*, Rahat Afrin†, Umair Manzoor*,†,¶, Arshad Saleem Bhatti‡, Mohammad Islam§, Muhammad T. Amin* and Abdulrahman A. Alazba*

*Alamoudi Water Chair, King Saud University,
P. O. Box 2460, Riyadh, Saudi Arabia
†Nano.Sensors.Catalysis@Department of Physics,
COMSATS Institute of Information Technology, Islamabad, Pakistan
‡Centre for Micro & Nano Devices, Department of Physics,
COMSATS Institute of Information Technology, Islamabad, Pakistan
§College of Engineering, King Saud University,
P. O. Box 800, Riyadh 11421, Saudi Arabia
¶umanzoor@ksu.edu.sa

Received 25 August 2014
Revised 19 March 2015
Accepted 23 March 2015
Published 21 August 2015

Multi-walled carbon nanotubes (CNTs) were grown via pyrolytic chemical vapor deposition technique and explored for their infrared sensing behavior. CNT synthesis was carried out over cobalt zinc ferrite ($Co_{0.5}Zn_{0.5}Fe_2O_4$) catalyst nanoparticles under different gas flow conditions to control outside diameter of the nanotubes. It was found that a progressive decrease in the carbon precursor gas (acetylene in this case) from 5:1 to 9:1 (v/v) causes reduction of average CNT diameter from 85 nm to 635 nm. Growth conditions involving higher temperatures yield nanotubes/nanofibers with outer diameter of >500 nm, presumably due to surface aggregation of nanoparticles or increased flux of carbonaceous species at the catalyst surface or both. Current–voltage characteristics of the nanotubes depending on the CNT diameter, revealed linear or nonlinear behavior. When incorporated as sensing layer, the sensitivity of ~ 5.3 was noticed with response time of ~ 4.1 s. It is believed that IR sensing characteristics of such CNT-based detectors can be further enhanced through post-synthesis purification and chemical functionalization treatments.

Keywords: CNTs; electrical properties; IR sensor.

1. Introduction

Carbon nanotubes (CNTs) are one-dimensional nanostructures, analogous to rolled graphene sheets into cylindrical shape, which gives them chirality and exhibit

¶Corresponding author.

sp^2 hybridization among covalently bonded carbon atoms.[1,2] In case of multi-walled carbon nanotubes (MWCNTs), the concentric cylindrical shells interact with each other through van der Walls forces.[3,4] Properties of CNT are very sensitive to their structure. CNTs can be metallic or semiconductors depending on their chirality.[5] Several factors influence the nanotubes diameter including catalyst nanoparticle size, growth temperature, gas mixture and growth time.[2] A strong correlation exists between the nanotube chirality and its diameter.[6] CNTs offer unique properties making them attractive for use in optical, thermal, chemical, mechanical, electrical, electromechanical and biological applications.[7–9]

Among several methods for synthesis of CNTs, chemical vapor deposition (CVD) technique offers certain advantages of low production cost,[1] high production yield,[10] scalability, growth on various substrates[11] and at much lower temperatures, to list a few.[12,13] During CVD process, the precursor source for carbon is pyrolytically decomposed and the subsequent influx of species at the nanoparticle surface promotes carbon dissolution and its supersaturation into the catalyst nanoparticle, thus leading to the crystallization of excess carbon in the form of cylindrical network with an outside diameter that corresponds to the average nanoparticle size. While there is heat generation, to a certain extent, owing to decomposition of the hydrocarbon gas, fraction of this heat is absorbed during carbon crystallization causing thermal gradient to develop inside the particle which keeps the process going.[14] Transition metals have been found to be efficient catalysts because of their high carbon solubility at elevated temperatures and high carbon diffusion rates. The presence of catalyst nanoparticles during CVD growth is critical to nucleation and subsequent nanotubes synthesis.[15]

In addition to a precursor gas for carbon, the use of argon gas prevents formation of amorphous carbon around nanosized catalyst particles beside controlling/reducing the CNT diameter. It also acts as a carrier or diluting agent to regulate growth kinetics through adjustment of acetylene decomposition rate.[12] In case of oxide nanoparticles, the hydrogen atoms produced from thermal decomposition reduce the metal oxide into pure metal, leading to slight reduction in size and surface activation for CNT growth.[10]

When used as radiation detectors, CNTs show wide absorbance and large photoresponse in the infrared spectral regime although a clear understanding of its origin is still not known.[16] For semiconductor CNTs, the band gap energy has values in the range of 0.4 eV and 6.0 eV,[17] there is an inverse relationship between the nanotubes diameter and band gap energy. The electronic configuration of CNTs depends on contribution from each individual shell making up the MWCNT structure.[18,19] The electronic properties of CNT are very sensitive to the geometric structure. Multi-wall nanotubes can be metallic or semiconducting depending upon the diameter which, in turn, is inversely proportional to band gap energies.[17] Morphology and specific properties of CNTs can be achieved by controlling different synthesis parameters.[20,21]

In this paper, we present our findings on CNT growth at various processing conditions of temperature and gas mixture ratios. Using mixed ferrites as catalyst nanoparticles and argon–acetylene gas mixtures, the influence of processing variables on nanotubes diameter was assessed followed by electrical characterization and determination of infrared (IR) radiation detection capabilities. Possible correlations between growth conditions, CNT characteristics and IR sensing behavior on CNT are discussed.

2. Experimental Procedure

CNTs were synthesized through CVD process with mixed ferrites as catalyst nanoparticles supported over silicon (100) surface and acetylene (C_2H_2) gas as carbon precursor source. Catalyst nanoparticles with the average size of ∼10 nm (iron-based compound $Co_{0.5}Zn_{0.5}Fe_2O_4$) were synthesized by chemical route and selected because iron-based catalysts usually produce carbonaceous tubes with high efficiency. A suspension of 0.15 g catalyst powder in 10 mL ethanol was sonicated for 10 min followed by taking a droplet of the suspension over clean silicon substrate surface. The catalyst loaded substrate was then inserted into a quartz tube (Φ 3.5 cm, length 100 cm) in a tube furnace. The nanoparticles supporting surfaces were heated to the synthesis temperatures of 730°C to 800°C at which C_2H_2 flow was maintained at 10 sccm for 25 min along with argon gas at a flow rate of 50, 70 or 90 sccm. Schematic illustration of CNT growth, as presented in Fig. 1, clearly demonstrates the experimental setup. Scanning electron microscope (SEM) examination was carried out to investigate the nanotubes morphology. The common practice of measuring the outer diameter of CNTs with the help of SEM results was followed, as suggested by many other independent researchers.[5–7,11,12] Also, extra care was taken and more than 80 measurements were averaged with best possible accuracy and precision.

For IR radiation detection, gold electrodes with a thickness of ∼100 nm were fabricated onto glass substrates (4×6 mm^2) via sputter deposition technique. The CNT scratched from Si support were applied to the spacing between electrodes by means of doctor blade apparatus. Both electrodes were connected to the sourcemeter (Keithley, model 2000) to measure any change in the electrical resistance (Fig. 2) while using a 100 W infrared lamp as IR radiation source.

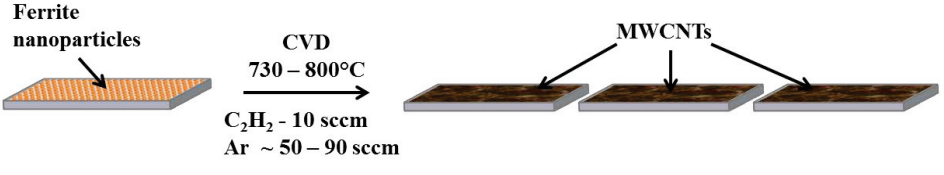

Fig. 1. Schematic representation of CNT synthesis setup.

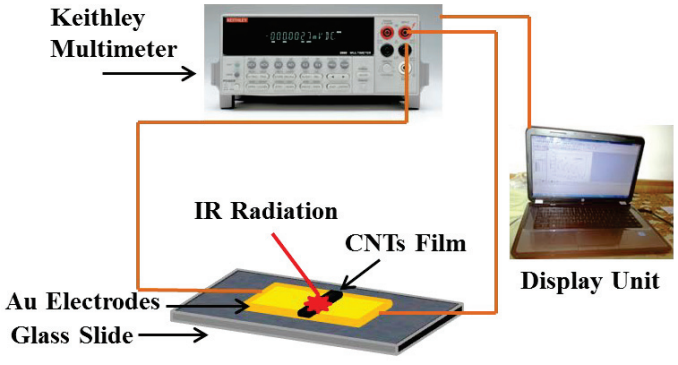

Fig. 2. Depiction of sensor configuration and IR radiation detection setup including source-meter and computer display.

3. Results and Discussion

Carbon nanotubes were produced via pyrolytic decomposition of C_2H_2 gas. The enthalpy change associated with C_2H_2 dissociation is large and negative, indicating the exothermic nature of the dissociation reaction. Since the reaction does not lead to net generation or consumption of gas, the entropy change is small and ΔG_r^0 changes only mildly with temperature. Although the $P_{H_2}/P_{C_2H_2}$ ratio, when plotted against temperature (Fig. 3), decreases with increasing temperature, yet it is independent of the total pressure. Thus, an increase in temperature does not favor the dissociation of acetylene. In other words, C_2H_2 decomposition is a kinetically

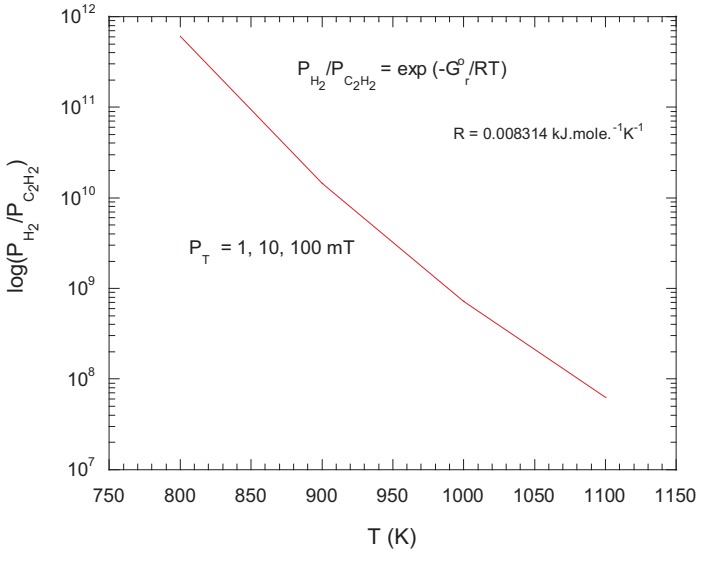

Fig. 3. Plot of T (K) versus log $(P_{H_2}/P_{C_2H_2})$.

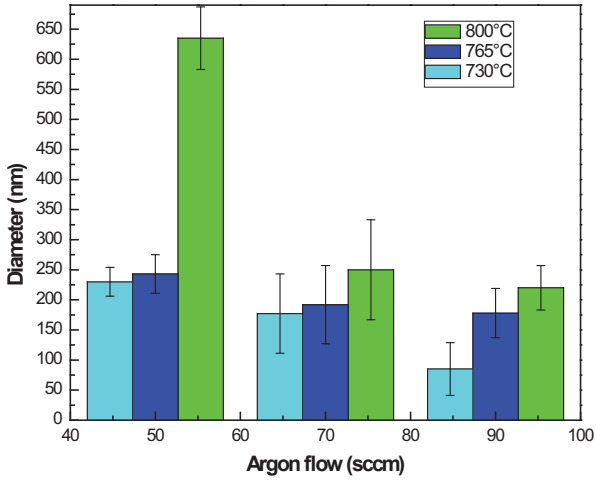

Fig. 4. Histograms showing the diameter distribution of CNTs for different mixture of argon and acetylene and at different temperatures.

controlled process. This is also evident from the fact that, for the same gas flow ratio, there is no drastic change in average outer diameter of the resulting MWCNTs. An increase in growth temperature from 730°C to 800°C, however, resulted in much greater degree of variation in the outer diameter. From SEM microstructures of the nanotubes shown in Fig. 4, the average CNT diameter is found to be in the range of $\sim$85 nm to 635 nm. For the same gas flow ratio, a progressive increase in the average diameter value was noticed. Such behavior may be attributed to an increased flux of carbonaceous species at the catalyst nanoparticle surfaces or nanoparticle clustering due to surface mobility at elevated temperatures followed by CNT growth or both.

As the argon to acetylene gas flow ratio (Ar:C_2H_2) is varied from 50:25 to 90:25 (sccm), the drop in carbon concentration at the nanoparticle surface causes marked decrease in the nanotubes diameter as manifested by an average value of 85 nm for CNT growth at 730°C. Since the initial catalyst nanoparticles have mixed spinal ferrite composition, it is anticipated that hydrogen produced upon C_2H_2 decomposition is utilized in reduction of these oxides into metallic state. Deposition of amorphous carbon beside nanotubes growth, in the form of spherical particles, few microns in diameter, is also observed after CNT growth at 765°C, 50:25 Ar:C_2H_2 [Fig. 5(d)] and 730°C, 90:25 Ar:C_2H_2 [Fig. 5(e)]. Thus, growth conditions of temperature and gas mixture flow investigated in this case influence nanotube/nanofiber diameter, area density and the amount of amorphous carbon co-deposited during CNT growth. Nanotube synthesis at conditions of lower temperatures (<700°C) and low total gas flow result in formation of a host of CNT morphologies, from straight to coiled.[6]

While assessing the effect of CNT growth temperature, we observe that the effect of C_2H_2:Argon flow rate ratio is most pronounced in case of synthesis at

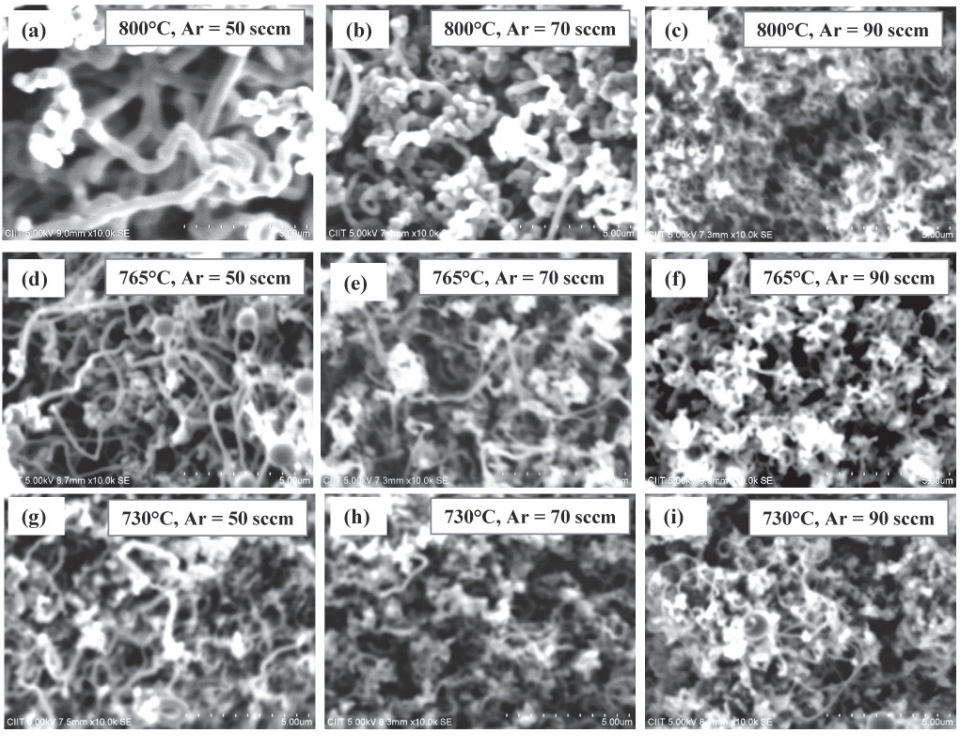

Fig. 5. SEM images of MWCNTs. The temperature and argon gas dependent diameter of CNTs are (a) 286 ± 152 nm, (b) 250 ± 183 nm, (c) 220 ± 137 nm, (d) 243 ± 30 nm, (e) 192 ± 65 nm, (f) 178 ± 41 nm, (g) 230 ± 24 nm, (h) 177 ± 66 nm and (i) 85 ± 44 nm. Bar size is 5 μm.

800°C [Figs. 5(a)–5(c)] with a progressive decrease in the average nanotubes outer diameter from > 500 nm to ~ 223 nm. This implies that dilution of C_2H_2 gas with argon promotes more homogeneity in the flux of carbonaceous species over the catalyst nanoparticles surface, thus leading to a higher CNT density. Enhanced surface mobility of the catalyst nanoparticles, possibly leading to clustering might be another reason for very large outer diameter. The reduction in CNT diameter upon dilution of a gas mixture is less drastic at lower growth temperatures. Under certain growth conditions, formation of amorphous carbon is also noticed [Figs. 5(d) and 5(i)], as indicated by open circles. Under all the synthesis conditions explored, the nanotubes growth occurred in a random fashion, giving a sphagetti-like appearance to the deposit. Due to high specific surface area of CNTs with low average outer diameter, their application as IR sensors makes an interesting research area. In order to produce CNT with small outer diameter values, a C_2H_2:Argon ratio of 25:90 is recommended for synthesis at all the temperatures.

The values of average nanotube diameter are presented as a histogram chart in Fig. 4. The CNT diameter values were calculated by averaging the diameter measurements for at least 30 individual CNTs. The error bars represent variation

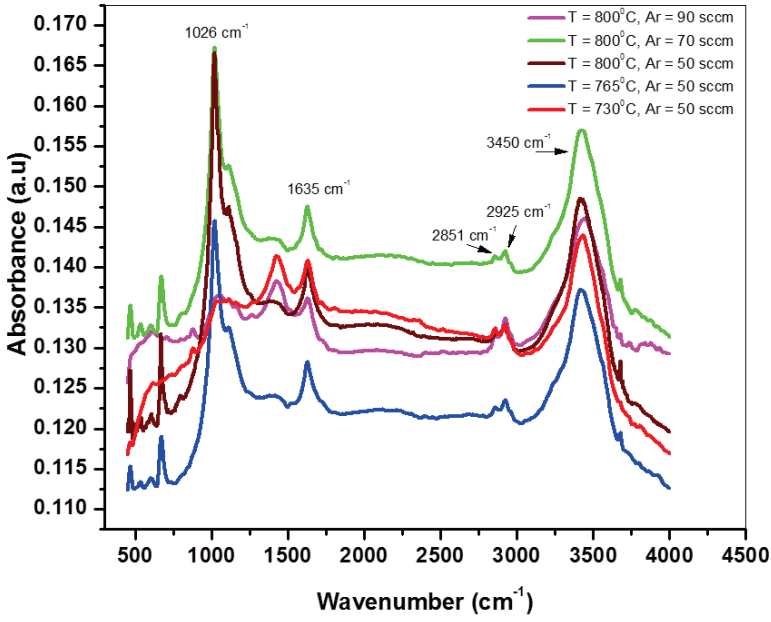

Fig. 6. (Color online) FTIR spectra of CNTs grown for different mixture of argon and acetylene and at different growth temperatures.

in CNT diameters produced from a particular set of growth conditions. The degree of variation in CNT diameter decreases upon dilution of C_2H_2 gas for all growth temperatures.

The difference in CNT characteristics was assessed by means FTIR spectroscopy studies of CNTs synthesized at different conditions, as shown in Fig. 6. The intense, sharp peak located at 1026 cm^{-1} is representative of Si–O stretching vibrations[8] and is caused by the Si substrate on which CNTs were grown. The broad peak present at 3450 cm^{-1} is characteristic of O–H stretching mode vibrations that can be attributed to the trace of water in the KBr pellet used for analysis. The weak shoulder peak at $\sim$3700 nm^{-1} (blue, brown and green spectra) may be attributed to the presence of free hydroxyl groups. The small, noticeable peaks at 2851 cm^{-1} and 2924 cm^{-1} correspond to the C–H asymmetric and symmetric stretching vibrations of the long alkyl chain. The stretching mode vibrations of the C=C bonds in the hexagonal network of CNT backbone structure gives rise to the peak at 1635 cm^{-1}.[14,16] The C–H bending mode vibrations of the alkyl chain cause formation of the peak at $\sim$1461 cm^{-1}, for red and pink spectra. The shoulder peak positioned at 1110 cm^{-1} for blue, brown and green spectra maybe attributed to the C–C–H symmetric bending. The four peaks in the 480–600 cm^{-1} spectral regime, seen in case of blue, brown and green spectra, maybe considered to be indicative of metallic/semi-metallic CNT structures while the rest of the transitions correspond to semiconductor structures.

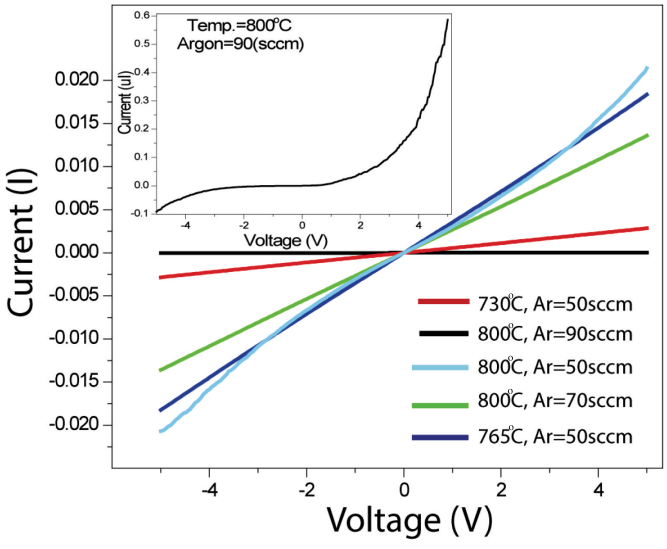

Fig. 7. (Color online) I–V curve of MWCNTs at the selected parameters.

The fact that van Hove singularities, an indicator of discrete density of states in one-dimensional structures, give rise to the presence of absorption bands in the spectral region from 480–600 cm^{-1}, it is possible that, under some of the growth conditions explored, MWCNTs with metallic structure and very small outer diameter were produced. In the absence of any post-synthesis purification or functionalization treatment, the similarity in IR spectra for blue, brown and green spectra indicate towards similar characteristics of CNTs grown at 765°C and 800°C temperature and high Ar:C_2H_2 ratio (50:25 or 70:25).

The electrical properties of the CNTs depend on their structure and chirality.[1] Upon IR irradiation, the current–voltage (I–V) behavior of the nanotubes, produced at different conditions, are presented in Fig. 7. It was observed that the CNTs produced at 800°C and 25:90 C_2H_2:Argon flow ratio exhibit linear behavior characteristic of small diameter CNTs. CNTs grown at 800°C having greater diameter showed semi-metallic behavior indicative of the presence of mixture of semiconducting and metallic CNTs. At this temperature, tunneling to inner tube shells and conduction through interbands and intrabands might be the major reasons for electrical transportation through CNTs.[6] CNTs grown at 730°C and 765°C having smaller diameter showed the linear behavior. The inset showed the magnified I–V curve of CNTs grown at 800°C and argon flow of 90 sccm. This nonlinear effect may be due to Schottky-diode behavior caused by formation of junctions between metal contact-CNT or metallic-semiconducting nanotubes. It is noteworthy that, in addition to the properties of the nanotubes, the electrical behavior arises from other factors also including, temperature,[22,23] inter- and intra-tube conductivity caused by solvent effects and tube/contact resistance.[24] The CNT growth

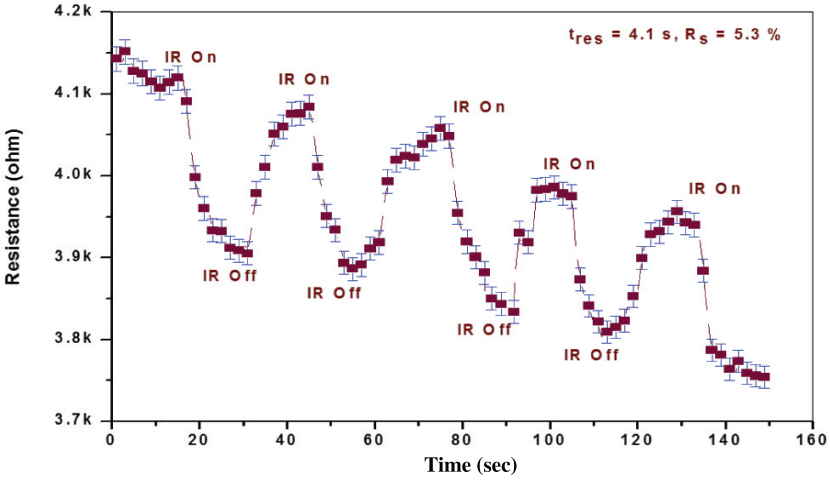

Fig. 8. Time-dependent changes in electrical resistance upon exposure to IR radiation for CNTs-based detectors made from randomly oriented nanotubes.

temperature has also been reported to influence transition from strong metallic to semi-metallic behavior upon synthesis at higher temperature.[25]

IR radiation sensing mechanism is related to energy absorption by the semiconducting CNTs and the subsequent change in electrical properties before and after IR radiation. At the onset of IR irradiation, the current rises immediately with an associated drop in the electrical resistance whereas the current falls back to its original value when the irradiation is switched off. This behavior is mainly because of photo-generated free charge carriers. The sensitivity "R_s" of different prototypes was measured using $\Delta R/R_0 = (R - R_0)/R_0$ where R is the maximum resistance before infrared illumination on the sample and R_0 is the minimum resistance after infrared illumination. The calculated average sensitivity of device was $R_s = 5.3\%$ and average response time was $t_{\text{res}} = 4.1$ s. There is a decrease in overall resistance with passage of time, this is due to the atmospheric and thermal effects (Bolometric effect). The overall thermal effect can be reduced at lowering sensor temperature.[6]

In summary, randomly oriented CNTs were successfully synthesized at different growth conditions. Morphological and structural study reveals the reduction of diameter of CNTs due to increase in inert gas concentration. We observed that diameter of CNTs can be controlled by dilution of hydrocarbon and it has a significant effect on growth of CNTs. Electrical properties showed the semimetallic behavior. The developed prototype sensors have good response towards IR radiations.

Acknowledgments

This project was funded by the National Plan for Science, Technology and Innovation (MAARIFAH), King Abdul Aziz City for Science and Technology, Kingdom of Saudi Arabia, Award Number (2623).

References

1. B. Xiang, Y. Zhang, T. H. Wang, J. Xu and D. P. Yu, *Mater. Lett.* **60** (2006) 754–756.
2. L. Stobinski, B. Lesiak, L. Kövér, J. Tóth, S. Biniak, G. Trykowski and J. Judek, *J. Alloys Compd.* **501** (2010) 77–84.
3. G. Trykowski, S. Biniak, L. Stobinski and B. Lesiak, *Acta Phys. Pol. A* **118** (2010) 515–518.
4. P. V. Kodgire, A. R. Bhattacharyya, S. Bose, N. Gupta, A. R. Kulkarni and A. Misra, *Chem. Phys. Lett.* **432** (2006) 480–485.
5. A. Misra, P. K. Tyagi, M. K. Singh and D. S. Misra, *Diamond Relat. Mater.* **5** (2006) 385–388.
6. R. Afrin, J. Khaliq, M. Islam, H. GulI, A. S. Bhatti and U. Manzoor, *Sensor Actuat. A* **187** (2012) 73–78.
7. A. Mahmoodi, M. Ghoranneviss, M. Mojtahedzadeh, S. H. Hosseini and M. Eshghabadi, *Int. J. Phys. Sci.* **7** (2012) 949–952.
8. Y. Tian, M. Y. Timmermans, M. Partanen, A. G. Nasibulin, H. Jiang, Z. Zhu and E. I. Kauppinen, *Carbon* **49** (2011) 4636–4643.
9. V. N. Popov, *Mater. Sci. Eng. R* **43** (2004) 61–102.
10. M. Kumar and Y. Ando, *J. Nanosci. Nanotechnol.* **10** (2010) 3739–3758.
11. M. Aksak, S. Kir and Y. Selamet, *J. Optoelectron. Adv. Mater. Symp.* **1** (2009) 281–284.
12. M. Aksak and Y. Selamet, *Appl. Phys. A* **100** (2010) 213–222.
13. Y. Homma, Y. Kobayashi, T. Ogino, D. Takagi, R. Ito, Y. J. Jung and P. M. Ajayan, *J. Phys. Chem. B* **107** (2003) 12161–12164.
14. K. S. V. Santhanama, R. Sangoia and L. Fullerc, *Sensor Actuat. B* **106** (2005) 766–771.
15. L. Pan, M. Zhang and Y. Nakayama, *J. Appl. Phys.* **91** (2002) 10058.
16. A. Gohier, A. Dhar, L. Gorintin, P. Bondavalli, Y. Bonnassieux and C. S. Cojocaru, *Appl. Phys. Lett.* **98** (2011), 063103.
17. M. S. Dresselhaus, G. Dresselhaus and P. Avouris, Electronics properties, junctions, and defects of carbon nanotubes, in *Carbon Nanotubes: Synthesis, Structure, Properties and Applications*, 1st edn. (Springer, Heidelberg, 2001), pp. 113–128.
18. C. F. Sun, B. Meany and Y. Wang, Characteristics and applications of carbon nanotubes with different numbers of walls, in *Carbon Nanotubes and Graphene*, 2nd edn., ed. K. T. Iijima (Elsevier, Oxford, 2014), pp. 313–339.
19. M. Inagaki, F. Kang, M. Toyoda and H. Konno, Carbon nanotubes: Synthesis and formation, in *Advanced Materials Science and Engineering of Carbon*, ed. M. I. K. T. Konno (Butterworth-Heinemann, Boston, 2014), pp. 15–40.
20. G. D. Nessim, A. J. Hart, J. S. Kim, D. Acquaviva, J. Oh, C. D. Morgan, M. Seita, J. S. Leib and C. V. Thompson, *Nano Lett.* **8** (2008) 3587–3593.
21. R. Xiang, G. Luo, Z. Yang, Q. Zhang, W. Qian and F. Wei, *Mater. Lett.* **63** (2009) 84–87.
22. J. Zhang, N. Xi and K. Lai, Fabrication and testing of a nano infrared detector using a single carbon nanotube (CNT), *SPIE Newsroom* (2007), doi:10.1117/2.1200701.0514.
23. N. Perera and P. Wijewarnasuriya, Improving microbolometric response using carbon nanotubes, Army Research Laboratory Report, ARL-TN-0523 (2013).
24. P. E. Pehrsson and J. W. Baldwin, Orientation, manipulation, and assembly of carbon nanotubes, Naval Research Laboratory Report, ARL, 2003.
25. C. Verissimo, S. A. Moshkalyov, C. S. Antonio, A. C. S. Ramos, J. L. Gonçalves, O. L. Alves and J. W. Swart, *J. Braz. Chem. Soc.* **17** (2006) 1124–1132.